

Hindawi Publishing Corporation  
Advances in Materials Science and Engineering  
Volume 2009, Article ID 502437, 4 pages  
doi:10.1155/2009/502437

## Research Article

# Structural and Raman Vibrational Studies of CeO<sub>2</sub>-Bi<sub>2</sub>O<sub>3</sub> Oxide System

L. Bourja,<sup>1,2</sup> B. Bakiz,<sup>1,2</sup> A. Benlhachemi,<sup>1</sup> M. Ezahri,<sup>1</sup> J. C. Valmalette,<sup>2</sup>  
S. Villain,<sup>2</sup> and J. R. Gavarri<sup>2</sup>

<sup>1</sup>Laboratoire Matériaux et Environnement LME, Faculté des Sciences, Université Ibn Zohr,  
BP 8106, Cité Dakhla, 80000 Agadir, Morocco

<sup>2</sup>Institut Matériaux Microélectronique et Nanosciences de Provence, IM2NP, UMR CNRS 6242,  
Université du Sud Toulon-Var, BP 20132, 83957 La Garde Cedex, France

Correspondence should be addressed to J. R. Gavarri, [gavarri.jr@univ-tln.fr](mailto:gavarri.jr@univ-tln.fr)

Received 10 August 2009; Accepted 1 November 2009

Recommended by Peter Majewski

A series of ceramics samples belonging to the CeO<sub>2</sub>-Bi<sub>2</sub>O<sub>3</sub> phase system have been prepared via a coprecipitation route. The crystallized phases were obtained by heating the solid precursors at 600°C for 6 hours, then quenching the samples. X-ray diffraction analyses show that for  $x < 0.20$  a solid solution Ce<sub>1-x</sub>Bi<sub>x</sub>O<sub>2-x/2</sub> with fluorine structure is formed. For  $x$  ranging between 0.25 and 0.7, a tetragonal  $\beta'$  phase coexisting with the FCC solid solution is observed. For  $x$  ranging between 0.8 and 0.9, a new tetragonal  $\beta$  phase appears. The  $\beta'$  phase is postulated to be a superstructure of the  $\beta$  phase. Finally, close to  $x = 1$ , the classical monoclinic  $\alpha$  Bi<sub>2</sub>O<sub>3</sub> structure is observed. Raman spectroscopy confirms the existence of the phase changes as  $x$  varies between 0 and 1.

Copyright © 2009 L. Bourja et al. This is an open access article distributed under the Creative Commons Attribution License, which permits unrestricted use, distribution, and reproduction in any medium, provided the original work is properly cited.

## 1. Introduction

In the past, several systems based on cerium dioxide CeO<sub>2</sub> (ceria) were extensively investigated for their electrochemical, conduction, or catalytic properties [1–15]. Nanostructured powders of pure and doped ceria can be obtained in various ways [16, 17]. In the present work we deal with the bismuth cerium oxide system CeO<sub>2</sub>-Bi<sub>2</sub>O<sub>3</sub>. This system might be of a high interest for catalytic applications and integration in gas sensors. At present, the cerium bismuth oxide phase diagram (CeO<sub>2</sub>-Bi<sub>2</sub>O<sub>3</sub>) is not well known. For low Bi fractions, it was clearly established that a solid solution was formed. The substituted phase Ce<sub>1-x</sub>Bi<sub>x</sub>O<sub>2-x/2</sub> (V)<sub>x/2</sub> with  $x < 0.20$  (where oxygen vacancies are noted V) is cubic and its cell parameter increases with  $x$  because of size of Bi<sup>3+</sup> ionic radius:  $r(\text{Bi}^{3+}) = 0.117 \text{ nm}$  and  $r(\text{Ce}^{4+}) = 0.097 \text{ nm}$  [18, 19]. However, above the composition  $x = 0.20$ , the nature of phases is not well known. In the present work, we describe a new series of observed phases prepared via a coprecipitation route and after heating at 600°C.

## 2. Experimental

Fourteenth polycrystalline samples were prepared by mixing bismuth and cerium nitrates solutions (Bi(NO<sub>3</sub>)<sub>3</sub>, 5H<sub>2</sub>O + Ce(NO<sub>3</sub>)<sub>3</sub>, 6H<sub>2</sub>O) and adding NH<sub>4</sub>OH [20, 21] to obtain precipitation of NH<sub>4</sub>NO<sub>3</sub> and bismuth cerium hydroxides. Bismuth compositions ranged from 0% Bi to 100% Bi. The solid obtained by coprecipitation was then heated under air at 600°C for 6 hours. Experiments carried out at intermediate heating times showed that the observed crystallized phases appear as being stable above heating times of 2 hours.

## 3. Results

The polycrystalline samples were analyzed by X-ray diffraction, using a D5000 Siemens-Bruker diffractometer, equipped with a copper X-ray source (wavelength  $\lambda = 1.54 \cdot 10^{-10} \text{ m}$ ; tension  $V = 45 \text{ kV}$ , intensity  $I = 35 \text{ mA}$ ), and with a monochromator eliminating  $K_{\beta}$  radiation. The

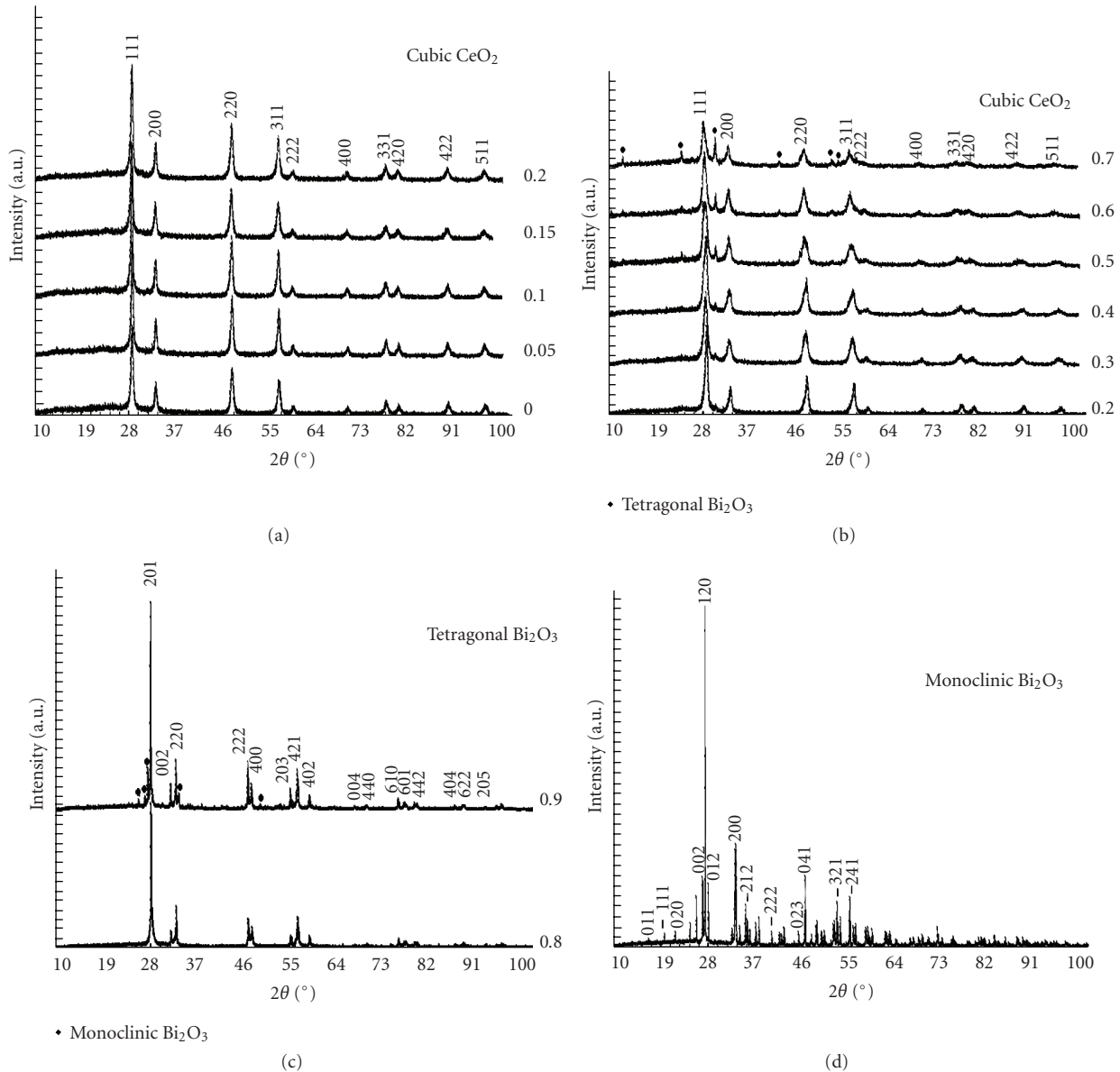


FIGURE 1: XRD patterns ( $\lambda_{\text{CuK}\alpha 1} = 1.54 \cdot 10^{-10}$  m) of pure samples  $(1-x)\text{CeO}_2$ ,  $x/2\text{Bi}_2\text{O}_3$  heated at  $600^\circ\text{C}$ . (a) XRD patterns for  $0 < x < 0.20$ ; (b) XRD patterns for  $0.25 < x < 0.70$  biphasic system; (c)  $x = 0.8$  and  $0.9$ ; (d)  $x = 1$   $\alpha$ - $\text{Bi}_2\text{O}_3$ .

analyses were carried out using the classical  $\theta$ - $2\theta$  configuration, with  $2\theta$  angle steps of  $0.02^\circ$  and counting times of 19 s per step. Raman spectroscopy was used to characterize the observed various phases. A micro-Raman system Horiba Jobin-Yvon Labram HR 800 equipped with argon laser source (Raman wavelength  $\lambda = 514.5$  nm) was used to observe the various vibrational spectra. All spectra were acquired with a recording time of 30 seconds.

**3.1. Structural Studies.** X-ray diffraction shows that a strong evolution occurs in the phase system as bismuth atom fraction increases. Figures 1(a), 1(b), 1(c), and 1(d) show the X-ray diffraction patterns for samples noted  $(1-x)\text{CeO}_2$ ,

$x/2\text{Bi}_2\text{O}_3$  with  $x$  varying between 0 and 1. The cell parameters of substituted samples  $\text{Ce}_{1-x}\text{Bi}_x\text{O}_{2-x/2}(\text{V})_{x/2}$  noted as  $a(x)$  were refined. From  $x = 0$  to  $x = 0.25$ , the cell parameters linearly vary with  $x$ :  $a(x = 0) = 0.5409 \pm 0.0001$  nm;  $a(x = 0.05) = 0.5413 \pm 0.0001$ ;  $a(x = 0.10) = 0.5417 \pm 0.0004$ ;  $a(x = 0.15) = 0.5419 \pm 0.0003$ ;  $a(x = 0.20) = 0.5421 \pm 0.0002$ .

Above the composition  $x = 0.20$ , a multiphase system is evidenced and the ceria-based phase presents a constant cell parameter  $a = 0.5421$  nm: the two new additional phases are identified as being tetragonal and closely related to bismuth oxide structural varieties: their cell parameters were refined. In the composition range from 0.3 to 0.7, a tetragonal  $\beta'$  phase is observed with refined cell parameters:

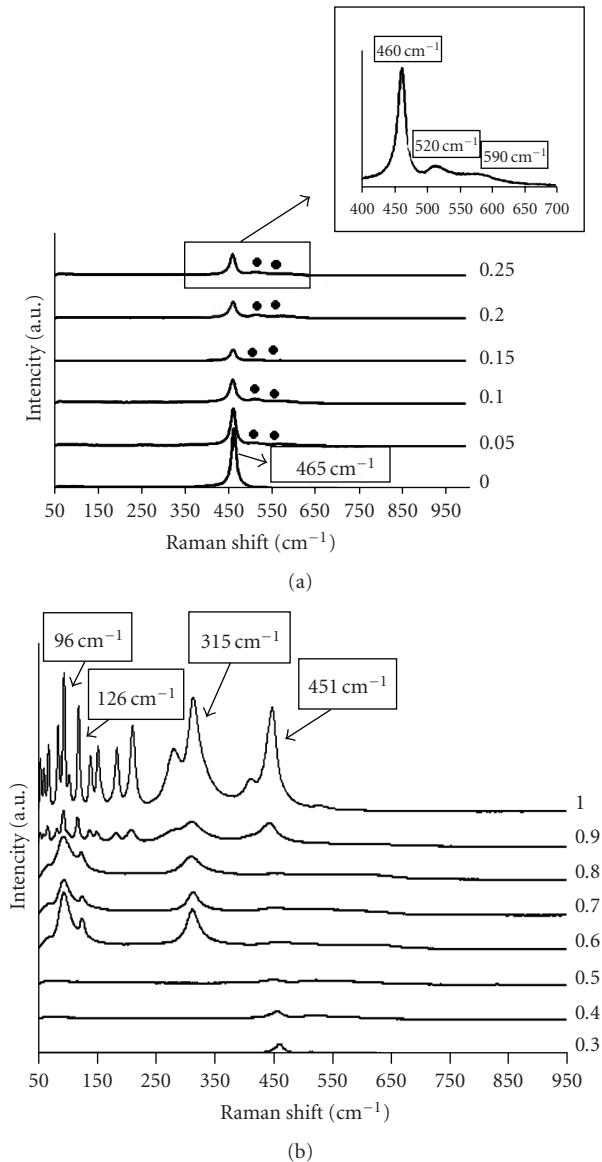


FIGURE 2: Raman spectra ( $\lambda = 514.5$  nm) of bismuth cerium oxide phases,  $(1-x)\text{CeO}_2, x/2.\text{Bi}_2\text{O}_3$ ; (a) solid solution for  $x = 0$  to 0.25; (b) multiphase system for  $x = 0.30$  to 1. Raman shift is in  $\text{cm}^{-1}$ ,  $x$  values from 0 to 1. The bands at 520 and  $590\text{ cm}^{-1}$  are linked to structural defects.

$a = 1.5542 \pm 0.0003$  nm;  $c = 0.5645 \pm 0.0001$  nm. It is a superstructure of the tetragonal  $\beta$  phase observed for compositions  $0.7 < x < 0.9$ , with refined cell parameters:  $a = 0.7742 \pm 0.0001$  nm;  $c = 0.5633 \pm 0.0001$  nm. These substituted phases were never observed, and testing structural models are in progress to better describe these phases.

3.2. *Vibrational Studies.* Raman spectroscopy data are reported on Figures 2(a) and 2(b): in Figure 2(a), the solid solution ( $0 < x < 0.25$ ) is characterized by a main vibrational band at  $460\text{--}465\text{ cm}^{-1}$  with complementary

small bands at  $520\text{--}590\text{ cm}^{-1}$  associated with the presence of  $\text{Bi}^{3+}$  and oxygen vacancies in the cubic lattice. In Figure 2(b) the Raman spectra of other samples are represented for  $x$  compositions ranging between 0.3 and 1. The vibration bands are increasingly more complex as Bi composition increases. The cubic phase of  $\text{CeO}_2$  is well characterized by the  $465\text{ cm}^{-1}$  Raman band. In the composition range from  $x = 0.05$  to 0.20 the bands located at  $462\text{--}516\text{--}595\text{ cm}^{-1}$  might be associated with the solid solution  $\text{Ce}_{1-x}\text{Bi}_x\text{O}_{2-x/2}$  ( $V$ ) $_{x/2}$ . The additional bands are underlined and should be linked to presence of  $\text{Bi}^{3+}$  ions and vacancies (clusters  $\text{Bi}^{3+}\text{-V-Bi}^{3+}$ ). In the range  $x = 0.30$  to 0.70, the Raman bands 460, 520, 590, 94, 126, 316, 530 ( $\text{in cm}^{-1}$ ) might be related to the biphasic system: cubic solid solution + tetragonal superstructure  $\beta'$ . In the range  $x = 0.80$  to 0.90, a new biphasic system associated with the bands 95, 120, 315, 450, 538 (tetragonal phase) and 70, 85, 140, 152, 184, 212, 285, 418, 630 (monoclinic lattice) is observed: these vibration bands could characterize the system "Tetragonal  $\beta$  + Monoclinic  $\alpha$ ." Finally for the  $\text{Bi}_2\text{O}_3$  sample, the standard  $\alpha$  monoclinic structure is observed.

#### 4. Conclusions


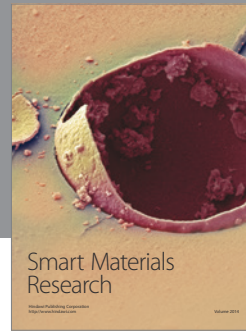
New correlations between XRD data and Raman spectroscopy have been established for the system  $\text{CeO}_2\text{-Bi}_2\text{O}_3$ . From samples prepared at  $600^\circ\text{C}$ , a partial phase diagram is proposed with the probable existence of at least 4 domains. The X-ray diffraction and Raman spectroscopy analyses clearly show that phase changes occur at  $600^\circ\text{C}$ , with at least (i) a solid solution domain (cubic phase), (ii) a biphasic domain (tetragonal phase  $\beta'$  rich in bismuth coexisting with the cubic phase), (iii) a biphasic system with coexistence of two  $\beta$  and  $\beta'$  tetragonal phases, the  $\beta$  phase being highly rich in bismuth, and finally (iv) a biphasic domain in which monoclinic and tetragonal  $\beta$  phases coexist. The solid solution can be represented from the basic  $\text{CeO}_2$  face-centered cubic lattice. The tetragonal phase  $\beta$  ( $x > 0.8$ ) can be represented by a cell built on the ceria fcc structure, with lattice vectors  $(a/\sqrt{2}, a/\sqrt{2}, a)$ : this structure was previously observed in the literature as a tetragonal variety of pure or non stoichiometric  $\text{Bi}_2\text{O}_3$  phase [22, 23]. The Bi rich phase ( $0.25 < x < 0.70$ ) having the superstructure noted  $\beta'$  can be represented by a cell built on lattice vectors  $(2a/\sqrt{2}, 2a/\sqrt{2}, a)$ . The observed pure  $\text{Bi}_2\text{O}_3$  phase is monoclinic. The effective compositions of the  $\beta$  and  $\beta'$  new cerium bismuth phases are not clearly known and new studies using transmission electron microscopy analyses are in progress.

#### Acknowledgment

The authors gratefully acknowledge the Provence-Alpes-Côte d'Azur Regional Council, the General Council of Var, and the agglomeration community of Toulon Provence Mediterranean for their helpful financial support in 2007 and 2008.

## References

- [1] J. Kašpar, P. Fornasiero, and M. Graziani, "Use of CeO<sub>2</sub>-based oxides in the three-way catalysis," *Catalysis Today*, vol. 50, no. 2, pp. 285–298, 1999.
- [2] A. Trovarelli, "Catalytic properties of ceria and CeO<sub>2</sub>-containing materials," *Catalysis Reviews: Science and Engineering*, vol. 38, no. 4, pp. 439–520, 1996.
- [3] A. Tschöpe, W. Liu, M. Flytzani-Stephanopoulos, and J. Y. Ying, "Redox activity of nonstoichiometric cerium oxide-based nanocrystalline catalysts," *Journal of Catalysis*, vol. 157, no. 1, pp. 42–50, 1995.
- [4] A. Tschöpe and J. Y. Ying, "Nanocrystalline cerium oxide catalytic materials," in *Nanophase Materials: Synthesis-Properties-Applications*, G. C. Hadjipanayis and R. W. Siegel, Eds., pp. 781–784, Kluwer Academic Publishers, Dordrecht, The Netherlands, 1994.
- [5] K. Bak and L. Hilaire, "Quantitative XPS analysis of the oxidation state of cerium in Pt-CeO<sub>2</sub>/Al<sub>2</sub>O<sub>3</sub> catalysts," *Applied Surface Science*, vol. 70–71, no. 2, pp. 191–195, 1993.
- [6] A. E. C. Palmqvist, E. M. Johansson, S. G. Järås, and M. Muhammed, "Total oxidation of methane over doped nanophase cerium oxides," *Catalysis Letters*, vol. 56, no. 1, pp. 69–75, 1998.
- [7] A. Martinez-Arias, M. Fernandez-García, O. Galvez, et al., "Comparative study on redox properties and catalytic behavior for CO oxidation of CuO/CeO<sub>2</sub> and CuO/ZrCeO<sub>4</sub> catalysts," *Journal of Catalysis*, vol. 195, no. 1, pp. 207–216, 2000.
- [8] G. Avgouropoulos and T. Ioannides, "Selective CO oxidation over CuO-CeO<sub>2</sub> catalysts prepared via the urea-nitrate combustion method," *Applied Catalysis A*, vol. 244, pp. 155–167, 2003.
- [9] H. C. Yao and Y. F. Yao, "Ceria in automotive exhaust catalysts. I. Oxygen storage," *Journal of Catalysis*, vol. 86, no. 2, pp. 254–265, 1984.
- [10] M. Mogensen, N. M. Sammes, and G. A. Tompsett, "Physical, chemical and electrochemical properties of pure and doped ceria," *Solid State Ionics*, vol. 129, no. 1, pp. 63–94, 2000.
- [11] T. J. Kirk and J. Winnick, "Hydrogen sulfide solid-oxide fuel cell using ceria-based electrolytes," *Journal of the Electrochemical Society*, vol. 140, no. 12, pp. 3494–3496, 1993.
- [12] P. Šulcová, "Synthesis of Ce<sub>0.95-y</sub>Pr<sub>0.05</sub>Nd<sub>y</sub>O<sub>2-y/2</sub> pigments," *Dyes and Pigments*, vol. 47, no. 3, pp. 285–289, 2000.
- [13] V. A. Sadykov, Y. V. Frolova, V. V. Kriventsov, et al., "Specificity of the local structure of nanocrystalline doped ceria solid electrolytes," in *Solid State Ionics*, vol. 835 of *Materials Research Society Symposium Proceedings*, pp. 199–204, 2004.
- [14] V. A. Sadykov, T. G. Kuznetsova, G. M. Alikina, et al., "Ceria-based fluorite-like oxide solid solutions as catalysts of methane selective oxidation into syngas by the lattice oxygen: synthesis, characterization and performance," *Catalysis Today*, vol. 93–95, pp. 45–53, 2004.
- [15] G. Li, Y. Mao, L. Li, S. Feng, M. Wang, and X. Yao, "Solid solubility and transport properties of nanocrystalline(CeO<sub>2</sub>)<sub>1-x</sub>(BiO<sub>1.5</sub>)<sub>x</sub> by hydrothermal conditions," *Chemistry of Materials*, vol. 11, no. 5, pp. 1259–1266, 1999.
- [16] N. Özer, "Optical properties and electrochromic characterization of sol-gel deposited ceria films," *Solar Energy Materials and Solar Cells*, vol. 68, no. 3–4, pp. 391–400, 2001.
- [17] S. Villain, Ch. Leroux, J. Musso, et al., "Nanoparticles and thin films of cerium dioxides: relations between elaboration process and microstructure," *Journal of Metastable and Nanocrystalline*, vol. 12, pp. 59–69, 2002.
- [18] V. Gil, C. Moure, P. Duran, and J. Tartaj, "Low-temperature densification and grain growth of Bi<sub>2</sub>O<sub>3</sub>-doped-ceria gadolinia ceramics," *Solid State Ionics*, vol. 178, no. 5–6, pp. 359–365, 2007.
- [19] S. Dikmen, P. Shuk, and M. Greenblatt, "Hydrothermal synthesis and properties of Ce<sub>1-x</sub>Bi<sub>x</sub>O<sub>2-δ</sub> solid solutions," *Solid State Ionics*, vol. 112, no. 3–4, pp. 299–307, 1998.
- [20] Z. Zhang, Y. Zhang, Z. Mu, et al., "Synthesis and catalytic properties of Ce<sub>0.6</sub>Zr<sub>0.4</sub>O<sub>2</sub> solid solutions in the oxidation of soluble organic fraction from diesel engines," *Applied Catalysis B*, vol. 76, no. 3–4, pp. 335–347, 2007.
- [21] Y. Ikuma, K. Takao, M. Kamiya, and E. Shimada, "X-ray study of cerium oxide doped with gadolinium oxide fired at low temperatures," *Materials Science and Engineering B*, vol. 99, no. 1–3, pp. 48–51, 2003.
- [22] F. D. Hardcastle and I. E. Wachs, "The molecular structure of bismuth oxide by Raman spectroscopy," *Journal of Solid State Chemistry*, vol. 97, no. 2, pp. 319–331, 1992.
- [23] A. J. Salazar-Pérez, M. A. Camacho-López, R. A. Morales-Luckie, et al., "Structural evolution of Bi<sub>2</sub>O<sub>3</sub> prepared by thermal oxidation of bismuth nano-particles," *Superficies y Vacío*, vol. 18, no. 3, pp. 4–8, 2005.



# Hindawi

Submit your manuscripts at  
<http://www.hindawi.com>

